ACCOUNTS of chemical research

Article

pubs.acs.org/accounts

The Renaissance of Halide Perovskites and Their Evolution as Emerging Semiconductors

Published as part of the Accounts of Chemical Research special issue "Lead Halide Perovskites for Solar Energy Conversion".

Constantinos C. Stoumpos and Mercouri G. Kanatzidis*

Department of Chemistry, Northwestern University, Evanston, Illinois 60201, United States

CONSPECTUS: The recent re-emergence of the halide perovskites, of the type AMX_3, derives from a sea-changing breakthrough in the field of photovoltaics that has led to a whole new generation of solar devices with remarkable power conversion efficiency. The success in the field of photovoltaics has led to intense, combined research efforts to better understand these materials both from the fundamental chemistry and physics points of view and for the improvement of applied functional device engineering. This groundswell of activity has breathed new life into this long-known but largely "forgotten" class of perovskites. The impressive achievements of halide perovskites in photovoltaics, as well as other optoelectronic applications, stem from an unusually favorable combination of optical and electronic properties, with the ability to be solution processed into films. This defines them as a brand new class of semiconductors that can rival or exceed the performance of the venerable classes of III−V and II−IV semiconductors, which presently dominate the industries of applied optoelectronics.

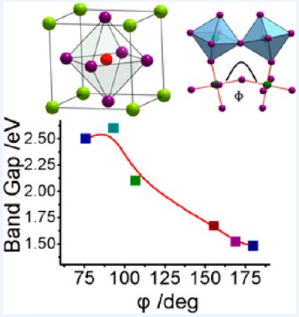

Our aim in this Account is to highlight the basic pillars that define the chemistry of the halide perovskites and their unconventional electronic properties through the prism of structure−property relationships. We focus on the synthetic requirements under which a halide perovskite can exist and emphasize how the synthetic conditions can determine the structural integrity and the bulk properties of the perovskites. Then we proceed to discuss the origins of the optical and electronic phenomena, using the perovskite crystal structure as a guide. Some of the most remarkable features of the perovskites dealt with in this Account include the evolution of a unique type of defect, which gives rise to superlattices. These can enhance or diminish the fluorescence properties of the perovskites. For example, the exotic self-doping ability of the Sn-based perovskites allows them to adopt electrical properties from semiconducting to metallic. We attempt to rationalize how these properties can be tuned and partially controlled through targeted synthetic procedures for use in electronic and optical devices. In addition, we address open scientific questions that pose big obstacles in understanding the fundamentals of perovskites. We anticipate that the answers to these questions will provide the impetus upon which future research directions will be founded.

1. INTRODUCTION

Groundbreaking recent discoveries that have truly brought the halide perovskites to the forefront of current research came (i) in 2009 when the hybrid halide perovskite, $CH_3NH_3PbI_3$, was demonstrated as a photosensitizer in a dye-sensitized solar cells (DSSCs);[1] this development caught up quickly and by 2012 halide perovskite photovoltaics (PV) were implemented in all-solid-state devices with $CH_3NH_3PbI_3$ playing a leading role as solar absorber[2−4] and (ii) when $CsSnI_3$ as a hole transporting material was used in a solid state DSSC.[5] Since then "perovskite solar cells" took off, and within a couple of years, the conversion efficiency of the devices sky-rocketed to ∼20%,[6,7] surpassing by a large margin the organic photovoltaics and rivaling established PV technologies based on Si, CdTe, $CuIn_{1-x}Ga_xSe$, and GaAs.

The aim of this Account is to illustrate the rich complexity of the halide perovskite semiconductors from the viewpoint of synthetic inorganic and materials chemistry but also highlight some of the main challenges in our understanding of these systems. We describe some of the fascinating properties of the compounds emphasizing their structural aspects and how these are related to their fundamental physical properties. The insights presented here arise mainly from the research experience gained in our group over the last five years on halide perovskite-based systems, driven by the desire to decipher the rules that govern the physical properties of this fascinating class of semiconductors.

2. THE PEROVSKITE (AND RELATED COMPOUNDS) CRYSTAL STRUCTURE

2.1. Crystal Structures

The perovskite crystal structure, AMX_3, is characterized by $[MX_6]^{4-}$ octahedra, which share corners in all three orthogonal directions to generate infinite three-dimensional (3D) $[MX_3]^-$ frameworks. The A^+ cations function as structural templates and their shape, size, and charge distribution are crucial factors for the stabilization of the perovskite structure (Figure 1). The

Received: May 4, 2015
Published: September 9, 2015

DOI: 10.1021/acs.accounts.5b00229
Acc. Chem. Res. 2015, 48, 2791−2802

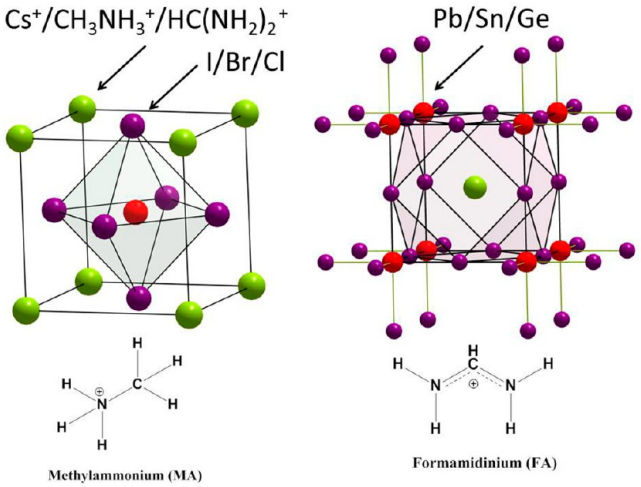

Figure 1. Crystal structure of the prototype AMX_3 perovskite emphasizing the corner-sharing connectivity of the $[MX_6]^{4-}$ units and the $[AX_{12}]^{11-}$ cuboctahedra.

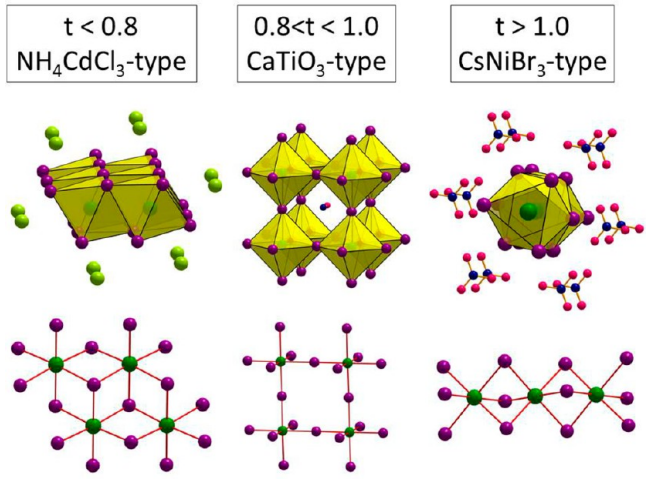

Figure 2. Established structural motifs for the AMX_3 halide compounds as a function of the ionic radii of A^+, M^{2+}, and X^- ions expressed with a tentative tolerance factor value.

rules that govern perovskite formation were tackled by Goldshmidt,[8] who introduced the namesake tolerance factor, $t = (r_A + r_X)/[\sqrt{2}(r_B + r_X)]$, where r_A, r_B, and r_X are the ionic radii of the respective ions in the AMX_3 formula.

Unlike their oxide counterparts, the $A^IM^{II}X^{-I}_3$ are much rarer and can only be formed with specific combinations of elements. This is because the halide (X^{1-}) anions (X = Cl, Br, I) impose two major differences in comparison to the oxide (O^{2-}) anion: (i) they bear a smaller negative charge, which is only sufficient to compensate metal ions in lower oxidation states, and (ii) they have a much larger ionic radii, which precludes the incorporation of small metal ions in octahedral coordination geometry. Because of these restrictions, the M^{II} metal anion can only be selected from a narrow set of elements including the alkaline earths,[9] the bivalent rare earths,[10] and the heavier group 14 elements (Ge^{2+}, Sn^{2+}, Pb^{2+}). Remarkably, there are no transition metals that can adopt the halide perovskite structure, with few notable exceptions.[11] The above considerations do not apply for $X = F^-$, which due to its small size can stabilize the perovskite structure for virtually all the bivalent metal ions.

Only three A cations known to date are able to stabilize the perovskite structure in heavy halides, Cs^+, $CH_3NH_3^+$ (MA), and $HC(NH_2)_2^+$ (FA). Whereas it is clear that Cs^+ is the only elemental cation that it is large enough to sustain the perovskite, for organic cations, it appears that it is not only size that is important but also the distribution of the net positive charge. Thus, $CH_3NH_3^+$ and $HC(NH_2)_2^+$ are able to stabilize the perovskite, but cations with similar size, such as $HONH_3^+$, $CH_3CH_2NH_3^+$,[12] or $(CH_3)_2NH_2^+$,[13] are not, stabilizing a different structure. When the cation is too small, the preferred structure is NH_4CdCl_3-type, which can be described as double chains of $[MI_5]^{3-}$. When the cation is too large, the preferred structure is $CsNiBr_3$-type, which consists of single-chains of face-sharing octahedra (Figure 2) On the other hand, too large, densely packed cations can give rise to perovskite-like structures albeit with a lower dimensionality.[14,15]

2.2. Structural Phase Transitions

The flexible nature of the perovskite framework, originating from the doubly bridging halide ion (M−X−M moiety), provides the perovskites with another trademark characteristic, successive phase transitions. Without exception, the perovskites undergo a series of structural changes upon application of external stimuli (temperature, pressure, etc.) starting from the ideal cubic archetype structure in which all M−X−M angles are 180° ($Pm\bar{3}m$ space group). This ideal structure responds to temperature or pressure changes by forcing the metal octahedra to tilt thereby lowering the symmetry in ways that depend on the characteristics of each compound (Figure 3). The tilting of octahedra does not change the overall 3D architecture but can significantly change the M−X−M angle from an ideal 180° to as low as ∼150°, below which the structure type changes or becomes amorphous.[16,17]

The physics of the phase transitions in perovskites is so diverse and exciting that it constitutes a research field of its own.[18−20] A detailed analysis of the problem lies outside the scope of this Account, and for the sake of clarity, we will use a simple approach by denoting the undistorted perovskite as the α-phase, the perovskite structure after the first phase transition as the β-phase, the perovskite after the second phase transition as the γ-phase, and the non-perovskite structure (either NH_4CdCl_3- or $CsNiBr_3$-sructure type) as the δ-phase, in line with the nomenclature used in our previous studies.[21] These phase transitions are fully reversible, even though in some cases the phase change can be kinetically blocked or the transition can be delayed up to several days. A characteristic example of these transitions is found in $CsMI_3$ (M = Sn, Pb) where the perovskite phases interplay with the non-perovskite isomers with the latter being the thermodynamically stable phases in ambient conditions (Figure 4).[22,23]

Although not strictly a phase transition, the benchmark halide perovskite $CH_3NH_3PbI_3$ can also adopt the δ-phases in the form of $CH_3NH_3PbI_3{\cdot}X$ solvates where any solvent with hydrogen bonding capability such as $X = H_2O$, DMF, DMSO, etc.,[24,25] can cause the collapse of the perovskite crystal lattice. This process is the origin of the apparent temporal instability in $CH_3NH_3PbI_3$ based solar cells. Remarkably, the solvation process in $CH_3NH_3PbI_3$ takes place at temperatures where the α/β phase transition also occurs (∼40 °C), suggesting a change of the transition pathway in the presence of certain solvents. Luckily, it has been shown that this destructive phase transition can be bypassed by maintaining the temperature above the

DOI: 10.1021/acs.accounts.5b00229
Acc. Chem. Res. 2015, 48, 2791−2802

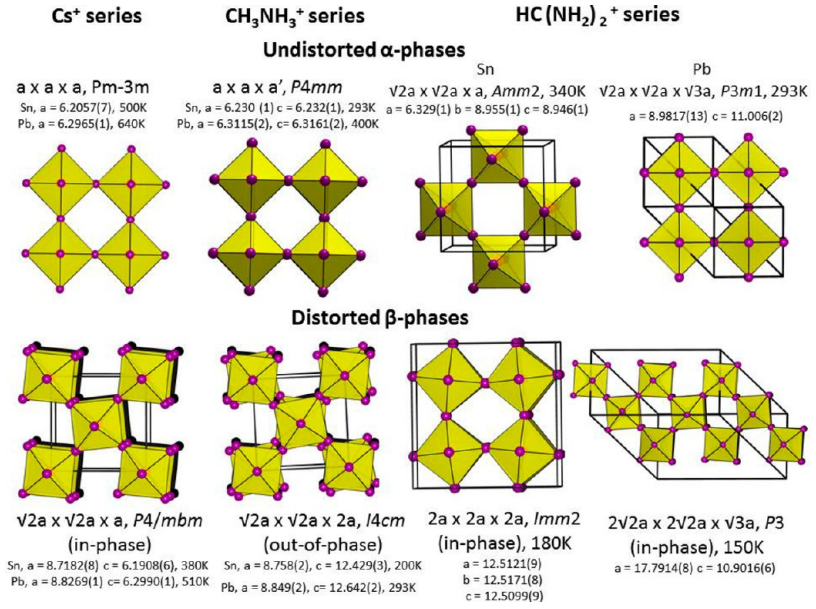

Figure 3. Crystal structures of halide perovskites following the sequential phase transitions from the undistorted α-phase to the distorted β-phases for the Cs, methylammonium, and formamidinium series, respectively.

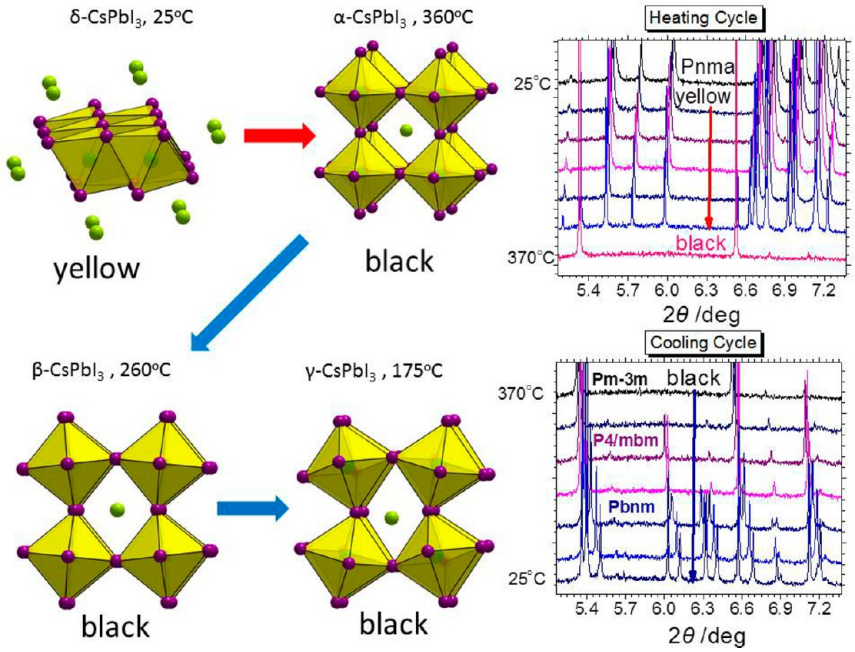

Figure 4. A case study of the phase transition scheme as observed with synchrotron powder diffraction (λ = 0.413906 Å) for the $CsPbI_3$ compound. Initially, the room temperature stable δ-phase (yellow) converts to the black perovskite α-phase upon heating above 360 °C. On cooling, the perovskite structure remains kinetically stabilized converting to the black perovskite β- and γ-phases at 260 and 175 °C, respectively. Full conversion of the γ- to the initial yellow δ-phase occurs after ~48h.

transition point during crystal growth[26] or using solvents with poor hydrogen bonding ability.[27]

3. OPTICAL PROPERTIES OF THE HALIDE PEROVSKITES

3.1. Band Gaps and the Role of the M–X–M Angle

One of the major reasons that the halide perovskites are excellent for photovoltaic applications is a very high absorption coefficient as recently demonstrated for β-$MAPbI_3$.[28] The sharp light absorption edge arises from a direct band gap transition. The band gaps of the perovskites are defined by the orbital overlap between the metal and the halide ions whereas the A cations do not directly contribute to the electronic properties.

Generally, in a given isostructural family of semiconductors with related elements (e.g., MQ where M = Zn, Cd; Q = S, Se, Te), the band gap decreases with increasing atomic mass. In the case of AMX_3 however, there is a strong anomaly where the Sn analogs have narrower bandgaps than the heavier Pb materials. This arises from the greater instability of the Sn^{2+} lone pair of electrons (residing in the s orbital), which in the octahedral coordination environment is pushed up in energy creating broader bands than the corresponding Pb lone pair. The latter

DOI: 10.1021/acs.accounts.5b00229
Acc. Chem. Res. 2015, 48, 2791–2802

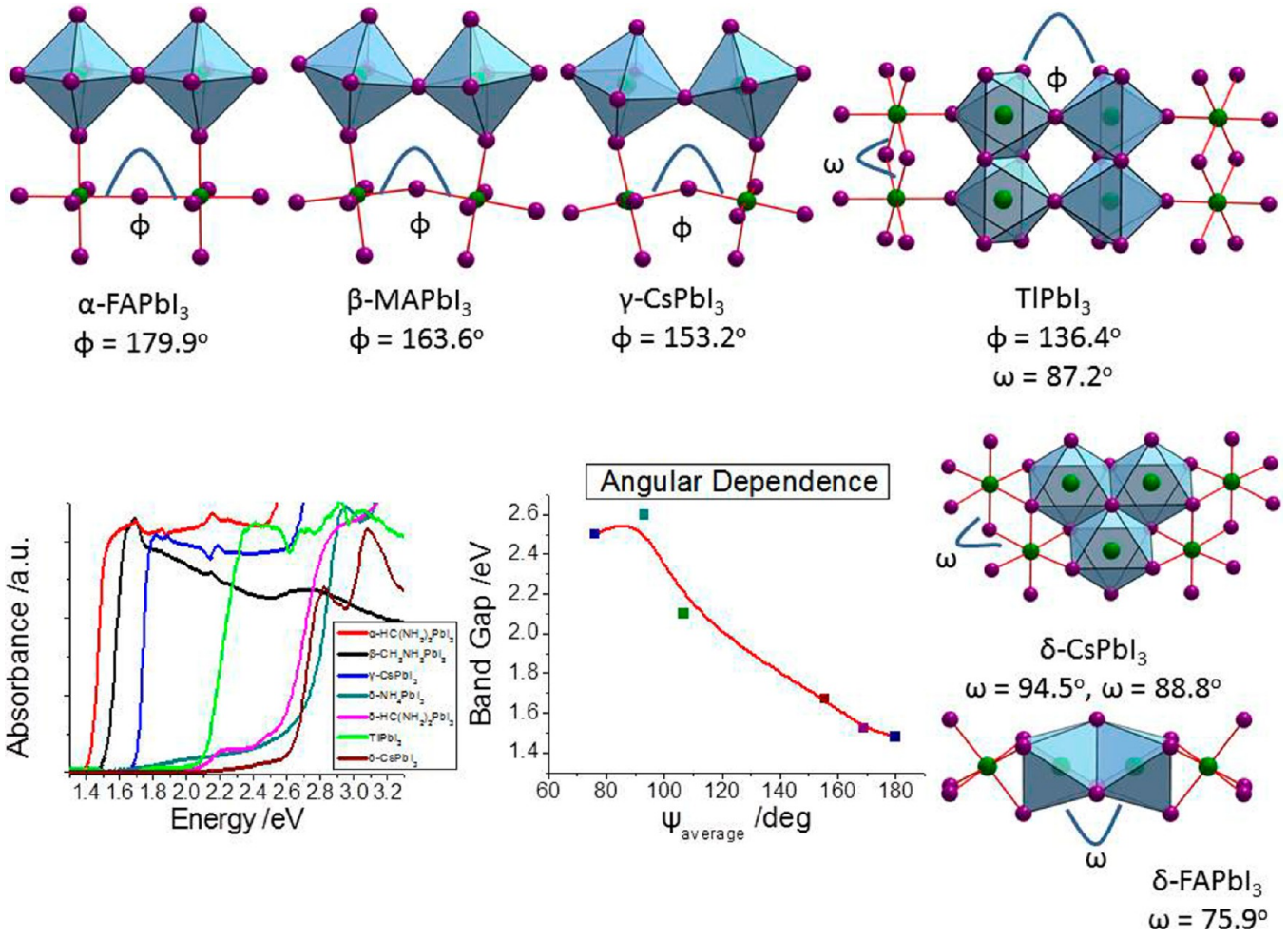

Figure 5. Experimental band gaps (from our laboratory) of the $APbI_3$ series at room temperature for A = FA, MA, Cs, Tl, and NH_4 cations highlighting the effect of the structural distortions and the connectivity of the $[PbI_6]^{4-}$ octahedra.

is not as spatially extended due to stronger relativistic effects. Thus, the band gaps of the Sn-based iodide perovskites, are narrower (1.2−1.4 eV) than those of Pb-iodide perovskites (1.45−1.7 eV).

Ideally, one would expect that all band gaps in a given AMX_3 series where "MX_3" is identical and only A changes to be very similar. However, this is not the case and the A cation has a strong influence on the band gaps. The A-cation contribution is indirect and lies in its structure directing role. Through steric and Coulombic interactions, it can deform the perovskite lattice in a cation-specific way. The octahedral tilting is then responsible for the changes in the electronic structure close to the band edges, which lead to the change in the band gap energetics.

A worked-out example of this trend is provided by the $APbI_3$ series. Starting with the perovskite forms, a clear trend can be observed in deviation from the ideal structure. The deviation from the ideal structure can be assessed by the M−X−M angle, ϕ, which decreases from α-$FAPbI_3$ to β-$MAPbI_3$ and to γ-$CsPbI_3$ (Figure 5). The deviation leads to an increase in band gap from 1.48 eV in α-$FAPbI_3$ to 1.67 eV in γ-$CsPbI_3$, and the degree of deviation can be quantified as a function of the ψ angle, which is defined as the average M−X−M angle in the "MX_3" framework. A similar concept can be also applied to the non-perovskite structures, which contain cations that do not stabilize the perovskite structure such as NH_4^+ and Cs^+ (NH_4CdCl_3-type) and FA^+ ($CsNiBr_3$-type). These non-perovskite structures display much wider gaps in the range of 2.4−2.6 eV, and in agreement with the concept, the M−X−M angles in these wide gap materials are much smaller ranging between ∼75° and 90°. (Even the "quasi-perovskite"$IIPbI_3$ follows this trend (2.1 eV)).

Solid solutions of halide perovskites can be prepared on both the M and X sites, but only as long as the M and X are immediate neighbors in the periodic table (Figure 6). For example, for a true $AMX'_{3-x}X_x$ solid solution, exemplified here by $CH_3NH_3SnI_{3-x}Br_x$, the absorption edge can be tuned between the two parent compounds (for x = 0 and x = 3, respectively) as a function of x following a simple linear relationship (Vegard's law). This systematic behavior is not observed in the "$CH_3NH_3SnI_{3-x}Cl_x$" composition, where instead of a continuous change in the absorption edge, a constant value is observed, which corresponds to that of $CH_3NH_3SnI_3$. This behavior, coupled with the X-ray diffraction data shows that this is a phase mixture of $CH_3NH_3SnI_3$ and $CH_3NH_3SnCl_3$.

The $AM'_{1-x}M_xX_3$ solid solutions are noteworthy as, for example, $CH_3NH_3Sn_{1-x}Pb_xI_3$,[21,29,30] which follows an irregular bandgap trend. Notably the band gaps of the solid solution are lower than the two parent compounds. This anomaly classifies the $CH_3NH_3Sn_{1-x}Pb_xI_3$ as a curiosity in the perovskite series for which further studies are required to understand the origins.

DOI: 10.1021/acs.accounts.5b00229
Acc. Chem. Res. 2015, 48, 2791−2802

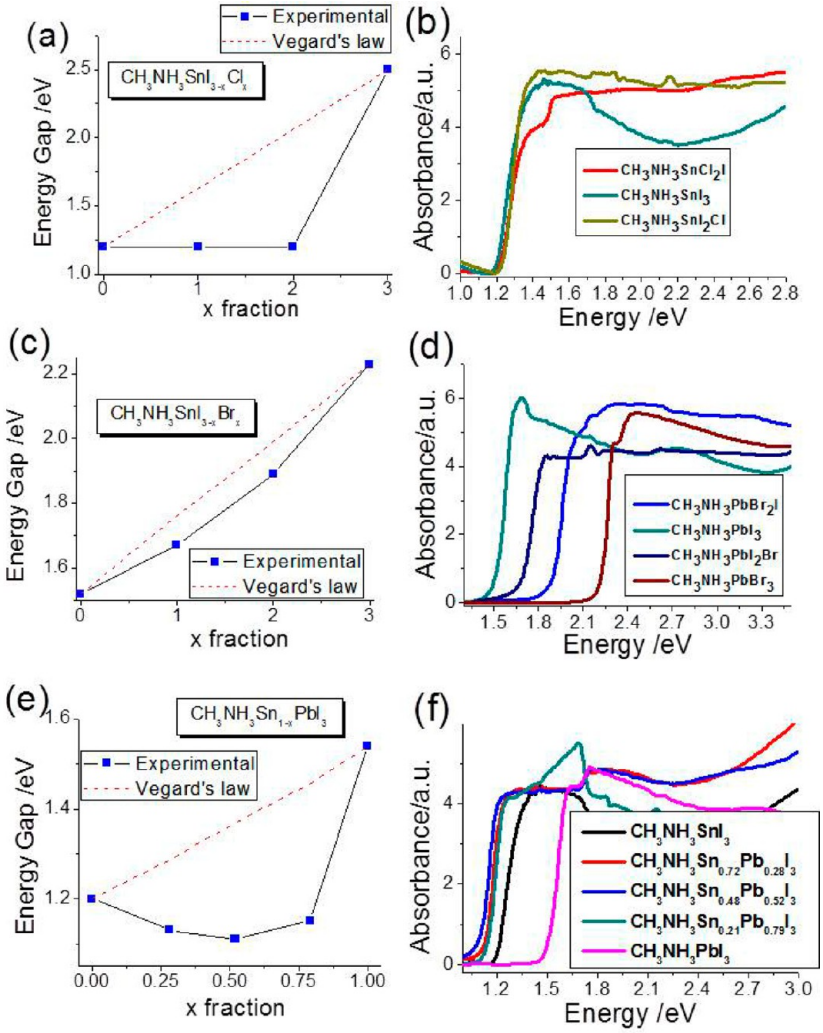

Figure 6. Dependence of the band gap (a, c, e) and the corresponding diffuse reflectance spectra (b, d, f) of the $MASnI_{3-x}Cl_x$ phase mixtures and of the regular $MAPbI_{3-x}Br_x$ and irregular $MAPb_{1-x}Sn_xI_3$ solid solutions, respectively. Reproduced in part from ref 21. Copyright 2013 American Chemical Society.

The mixing of Sn and Pb metal ions in itself does not introduce any significant change in the crystal lattice, but instead it triggers a composition-directed phase transition at room temperature from the α-phase of $CH_3NH_3Sn_{1-x}Pb_xI_3$ present for $0.0 < x < 0.5$ to the β-phase for $0.5 < x < 1.0$. Theoretical calculations indicate the origin of the anomalous band gap occurs due to antagonistic effects that act simultaneously on the electronic structure: (i) a bandgap reduction caused by strong spin−orbit coupling (SOC) interactions, which are dominant in the $0.0 < x < 0.5$ range and (ii) the bandwidth decrease (which increases bandgap) caused by the lattice distortion as a function of x and is dominant in the $0.5 < x < 1.0$ compositional range.[31] As a result of this anomalous trend, we were able to fabricate functional photovoltaic devices that were able to absorb light up to ca. 1050 nm (lowest energy achieved yet) and at the same time display superior current characteristics with respect to $CH_3NH_3PbI_3$ as a result of the Sn incorporation in the lattice (Figure 7).[29] We foresee further paths for property tuning based on unconventional trends in electronic structure of perovskites.

3.2. Photoluminescence (PL) Properties

As direct band gap semiconductors, the halide perovskites can display photoluminescence (PL) even at room temperature. However, in contrast with the absorption properties, the PL properties do not always express themselves. The PL emission can be always observed at cryogenic temperatures, but at room temperature, the emergence of PL emission shows a strong dependence on the synthesis method of the perovskite. Here we focus on the room temperature PL properties since most relevant applications of perovskites are associated with their properties under ambient conditions. For example, very strong PL is always observed in thin-films[3] and matrix embedded nanocrystals,[32] but it is absent when the bulk material is prepared in hydrohalic acid solution. Because of the room temperature PL at tunable wavelengths in the visible spectrum and (in the case of the Sn-based materials) in the near-infrared region, such materials have been proposed for laser applications[33] and radiation detectors,[34] respectively. However, in the bulk materials, the PL property is largely dependent on the method of synthesis.[21] For example, samples prepared by us in HI/H_3PO_2 solution display no PL activity. However, when the materials are prepared by solid-state chemistry methods even by just grinding the reactants at room temperature, strong

DOI: 10.1021/acs.accounts.5b00229
Acc. Chem. Res. 2015, 48, 2791−2802

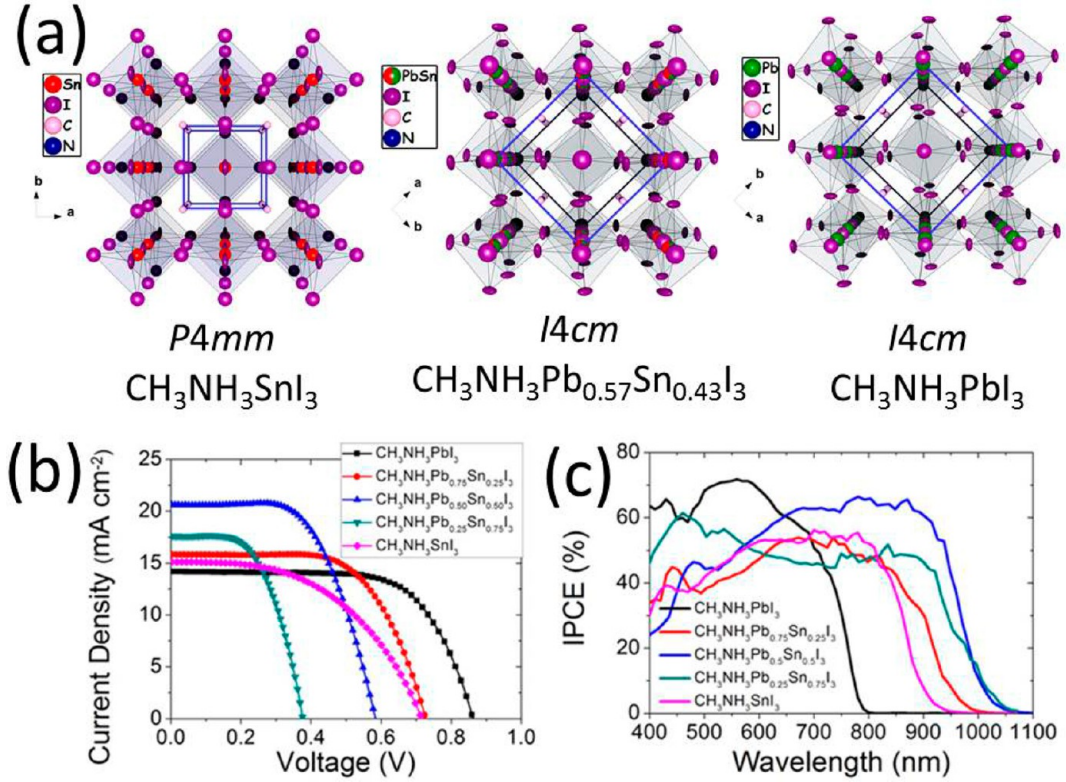

Figure 7. $CH_3NH_3Sn_{1-x}Pb_xI_3$ solid solutions: (a) crystal structure, (b) photocurrent $J-V$ device characteristics, and (c) photovoltaic quantum efficiency as a function of composition. Reproduced with permission from ref 29. Copyright 2014 American Chemical Society.

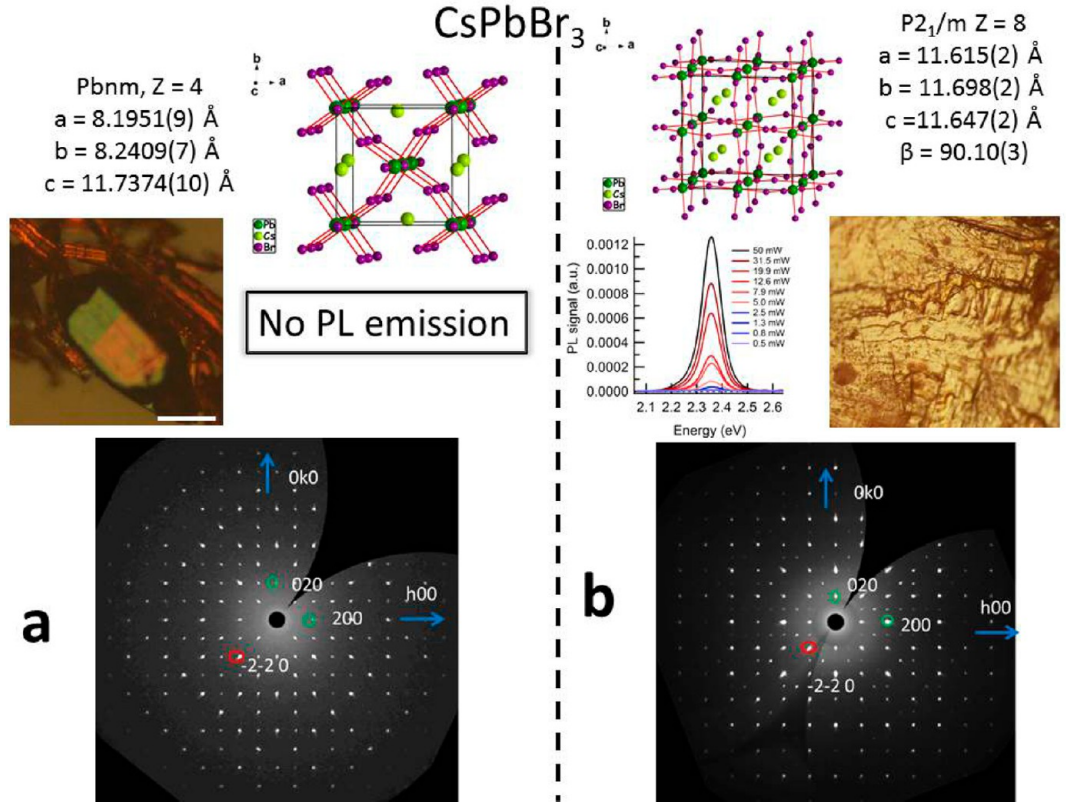

Figure 8. Crystal structures, simulated precession diffraction images of the (110) planes, photographs, and PL properties of (a) HBr/H_3PO_2 solution grown and (b) solid-state grown crystals of $CsPbBr_3$. The scale bar of the photographs is 100 μm.

DOI: 10.1021/acs.accounts.5b00229
Acc. Chem. Res. 2015, 48, 2791−2802

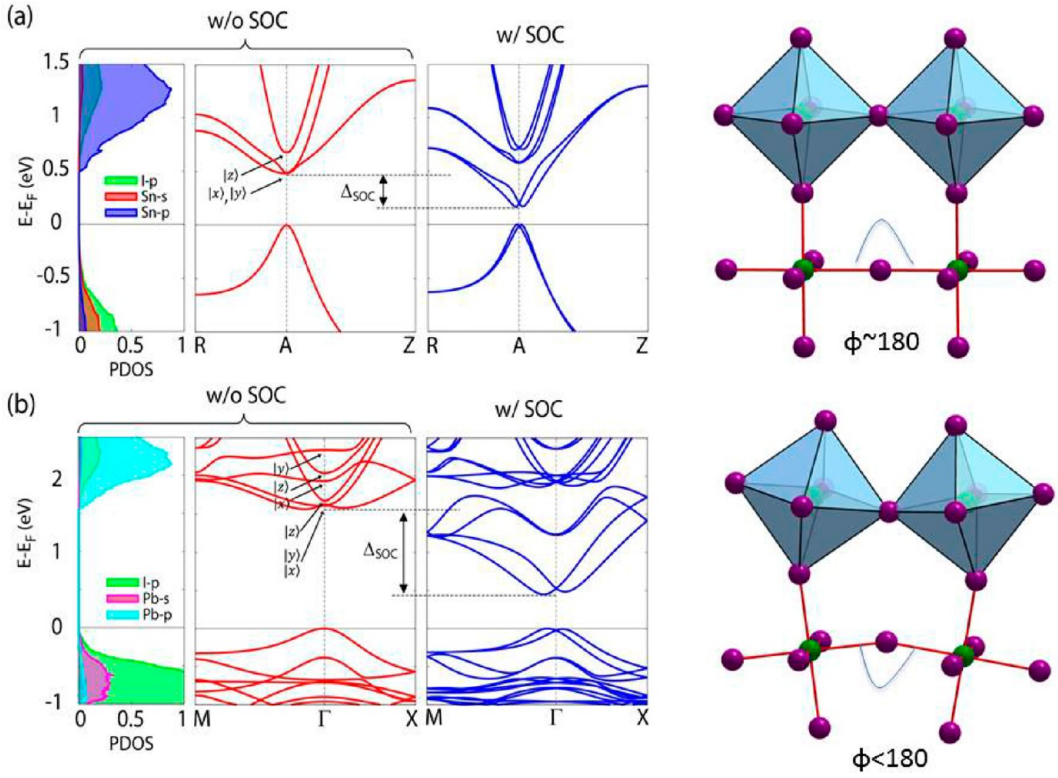

Figure 9. Electronic band structure of α-$MASnI_3$ and β-$MAPbI_3$ highlighting the evolution of the electronic structure of perovskites upon the structural phase transition. The corresponding crystal structures are shown for comparison, illustrating the effect of octahedral tilting in the band shape close to the valence band maximum (VBM) and conduction band minimum (CBM) regions. Reproduced with permission from reference 31. Copyright 2015 American Chemical Society.

PL is observed. This trend seems to be related to defects and impurities introduced in the various synthetic processes, which are responsible for switching on and off the emission properties. Currently, understanding the origin of PL and its relationship to sample quality is lacking. The widely accepted model is that the halide perovskites display direct gap band-to-band emission originating from the transition between the conduction and valence bands of the semiconductors, however, we believe that these phenomena is more complicated than this simple view. What is truly remarkable in the case of $ASnI_3$ is the coexistence of PL and high electrical conductivity, two properties presumed to be mutually incompatible.

A representative case-study is $CsPbBr_3$, a wide gap semiconductor (E_g = 2.25 eV) that we have investigated as a potential material for hard radiation detection.[35] The crystals display PL emission at 2.37 eV (523 nm) at room temperature; however, the intensity ranges up to 3 orders of magnitude among samples with different degrees of purity. The large variation in PL shows that the carrier generation and recombination processes are very complex and the PL most likely arises from defects. Interestingly $CsPbBr_3$ crystals grown from acid solution below the transition temperature (~120 °C) do not show room temperature PL. This discrepancy can be traced all the way to the crystal structure where we found that the "solid-state prepared" crystals consistently display signature reflections of a nearly cubic but monoclinic superlattice that is four times larger than the proper orthorhombic unit cell. By contrast, the crystals grown at ambient temperature do not show the superlattice (Figure 8).

At this stage, it is not clear whether PL in the $ASnX_3$ and $APbX_3$ materials comes from structure defects or the band edge. Although there are several synthetic methods for preparing these materials, we do not understand which method results in what defects. We need additional studies to recognize and quantify the nature of the defects and determine which synthesis method gives samples with the lowest number of them. Therefore, more sophisticated experiments will be required to validate the lattice defect concept and understand the origin of PL.

4. ELECTRONIC AND ELECTRICAL PROPERTIES OF THE HALIDE PEROVSKITES

4.1. Electronic Band Structure

The optical absorption of AMX_3 perovskites is believed to be typical of direct band gap semiconductors. Theoretical calculations universally confirm this for all the M = Ge, Sn, or Pb and X = Cl, Br, or I members.[36−40] These studies also show that as the perovskites transition from the α- to the β- and the γ-phases, the bandwidth narrows in favor of the increased density-of-states (DOS) on top of the valence band and the band gap increases (Figure 9). This can be intuitively understood by visualizing the overlap between the orbitals of M and X. In the ideal undistorted perovskite crystal structure, the axial orbital overlap between the halide p-orbitals and the metal s- and p-orbital is optimal, and this overlap leads to a significant broadening of the s-type valence band thus significantly increasing the width of the band and narrowing the band gap. As the octahedra begin to tilt, the axial orbital mixing weakens leading to a decrease of bandwidth. We therefore expect the optimal electronic properties to be in the higher symmetry modifications of perovskites with as linear a

DOI: 10.1021/acs.accounts.5b00229
Acc. Chem. Res. 2015, 48, 2791−2802

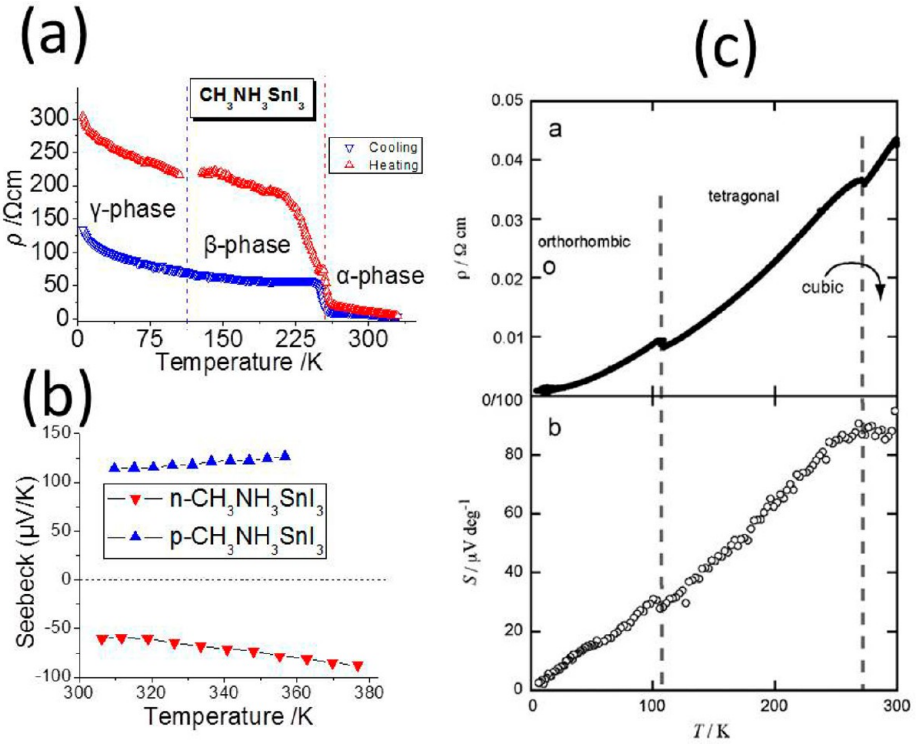

Figure 10. Electrical properties of $CH_3NH_3SnI_3$ perovskite indicating their sensitivity to preparation method. (a) Temperature-dependent resistivity of a single-crystal sample prepared from HI/H_3PO_2 solution. The magnitude and temperature dependence is typical of a semiconductor. The anomalies in resistivity correspond to the temperature where the structural transitions take place. (b) Temperature-dependent Seebeck coefficients for a polycrystalline sample prepared by annealing at 200 °C under vacuum (n-type) and a polycrystalline sample prepared by annealing at high temperature in air (p-type). Reproduced with permission from ref 21. Copyright 2013 American Chemical Society. (c) Temperature-dependent resistivity and Seebeck coefficient of a single-crystal sample prepared from a HI solution.[45] Clearly, this sample is hole doped and exhibits metallic properties. Reproduced with permission from ref 45. Copyright 2013 Elsevier.

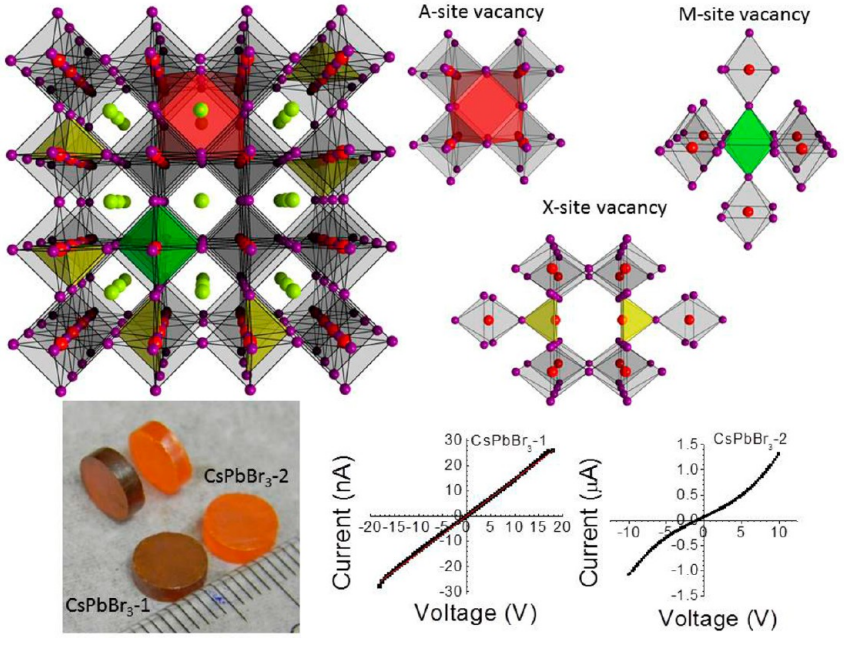

Figure 11. Schottky defect model in the halide perovskites. A $4 \times 4 \times 4$ superlattice of the cubic AMX_3 perovskite lattice where 1/64 of the formula unit has been removed creating random localized defects. A case-study of how the defects affect the properties is shown for single-crystals of $CsPbBr_3$ prepared from commercial ($CsPbBr_3$-1) or homemade ($CsPbBr_3$-2) precursors with the crystals displaying different color intensity. The optical gap for the two compounds is identical but the electrical response shown in the $I-V$ plots is different.

M−X−M angle as possible, a trend confirmed by the electrical properties of the compounds (see below).

DOI: 10.1021/acs.accounts.5b00229
Acc. Chem. Res. 2015, 48, 2791−2802

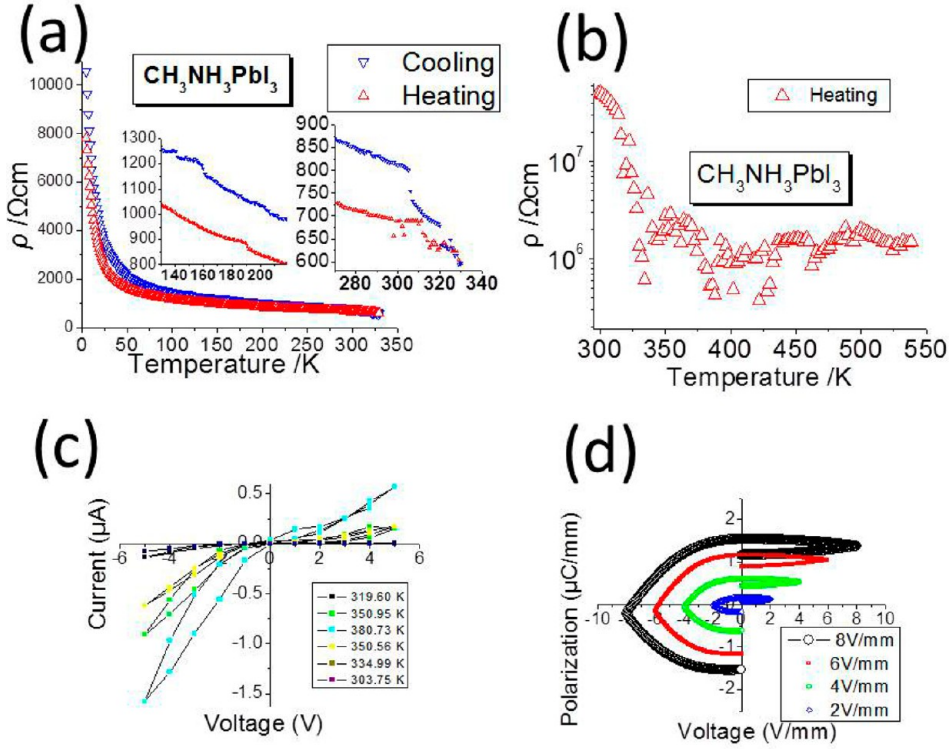

Figure 12. Electrical properties of the $CH_3NH_3PbI_3$ perovskite. (a, b) Electrical resistivity data showing the impact of the phase transitions appearing as anomalies in the ρ vs T plots. The insets in panel (a) highlight the temperature at which the structural transitions take place. (c) $I-V$ plots as a function of temperature displaying an increasing degree of hysteresis and irreversibility with increasing temperature. (d) Polarization vs electric field plots implying ferroelectric-like behavior at room temperature. Reproduced with permission from ref 21. Copyright 2013 American Chemical Society.

4.2. Charge Transport Properties

The electrical properties of halide perovskites have always been a source of both excitement and controversy. It has been proposed in several instances that the electrical properties are ionic in origin, arising from movement of halide ions.[41,42] However, others reported consistently metallic behavior in $ASnI_3$, pointing toward an electronic charge transport mechanism.[43−47] A careful examination of the previous work reveals that a wide range of preparation methods have been employed, which may well explain such conflicting results. Our own experience with the tin halide perovskites has taught us that they can be made either metallic or semiconducting depending precisely on the preparation method.[21,23] Briefly, when the tin materials are made from high temperature melts, we observe metallic p-type behavior. By contrast, under low temperature synthesis conditions, we could obtain n-type nearly intrinsic semiconductors (Figure 10).

The case of lead perovskites is different since the self-doping process from oxidation of Pb^{2+} to Pb^{4+} is energetically unfavorable, and as a result the Pb-based perovskites always behave as intrinsic semiconductors. Nevertheless, it has been shown recently that even in the case of lead, the method of preparation can lead to completely different electrical properties.[26,27,48]

The ionic component of the halide perovskites may be enhanced by the sequential phase transitions, which can initiate the displacement of certain atoms from their designated positions in the lattice and create local charged defects. The charged defects can generate electrostatic potentials, which will locally influence the carrier density but without changing the stoichiometry of the material. Therefore, it seems reasonable that the best material quality can be obtained either by synthetic methods that allow for a dynamic redistribution of the ions within the structure such as solution growth, where the crystals are dissolved and formed again, or by extensive annealing where misplaced atoms relocate to their ideal positions. Incidentally, the samples prepared by these methods do not display PL at room temperature, as discussed above, which is another indication that controlling the Schottky-type defects in the materials can play a crucial role in directing the optical and electrical properties of the compounds (Figure 11).

Accurate carrier density determination in perovskites is challenging. For $MASnI_3$, the metal-like form of the compound prepared from HI acid solution under inert atmosphere or film-deposited under vacuum (containing Sn^{4+} dopants)[43,45] has carrier concentration of $\sim 10^{19}$ cm^{-3} in line with a similar result obtained by us for doped samples of $CsSnI_3$.[23] However, for n-type samples obtained through a H_3PO_2/HI mixture under nitrogen (to suppress oxidation of Sn^{2+}) or by annealing at 200 °C under vacuum (to remove the volatile SnI_4), the carrier concentrations were estimated in the $10^{13}-10^{15}$ cm^{-3} range (virtually in the intrinsic semiconductor regime). These samples display a typical semiconducting trend in electrical conductivity.

The estimation of mobility using $\mu = 1/(ne\rho)$ gave high values for bulk $MASnI_3$, which, however, could not be observed in the thin-film form of the perovskite using terahertz spectroscopy measurements.[49] Instead, a recent Hall effect measurement on $CsSnI_3$ thin-films[50] suggests $n \approx 10^{17}$ cm^{-3} carrier density in line with our previous measurements for the bulk $CsSnI_3$ metal-like semiconductor.[23] At our current level of

DOI: 10.1021/acs.accounts.5b00229
Acc. Chem. Res. 2015, 48, 2791−2802

understanding, we attribute this discrepancy to peculiarities of the Sn-based perovskites rather than in deficiencies of our experimental method since the same measurements performed on $MAPbI_3$ samples are in fair agreement with those obtained from terahertz spectroscopy ($\mu \approx 25$ cm^2/(V s) (THz) vs $\mu \approx 66$ cm^2/(V s) (Hall)).[51] Based on these observations, the greatest challenge in terms of photovoltaics—applications of Sn-based perovskites lies in the successful deposition of thin-films with low carrier density. This should be a main research goal if Sn-based PV devices with high efficiency are to be realized.[52]

The electrical charge transport measurements are a useful characterization tool for the materials and devices since they are very sensitive to structural phase transitions (Figure 12). Using single-crystals of $MAPbI_3$, we have found a significant drop in resistivity as the β-phase changes to the α-phase, between 40 and 60 °C. Thus, the initial resistivity value of $MAPbI_3$ abruptly drops upon the phase change from 51 to 6.0 MΩ·cm. This drop is attributed to a jump in mobility and is in good agreement with the electronic structure calculations, discussed above. Such considerations are in line with recent developments in perovskite solar cells where a record efficiency has been reached by employing the $(FAPbI_3)_{1-x}(MAPbBr_3)_x$ compositions, which stabilize the α-phase of the perovskite.[7] Finally, we highlight the appearance of ubiquitous hysteresis behavior in current—voltage scans of samples of $MAPbI_3$ regardless of phase they are in. This hysteresis is demonstrated by the temperature-dependence of $I-V$ curves and polarization measurements (Figure 12c,d). The hysteresis behavior is also consistently observed in most $J-V$ curves of solar cell devices,[53] and one of the possible explanations may be the presence of ferroelectricity or the dynamic behavior of atoms in the perovskite.

5. CONCLUSIONS AND OUTLOOK

The emergence of ternary halide perovskites as a new class of remarkable semiconductors has strongly stimulated the scientific community in the past few years. These "old" materials with exciting, puzzling, and often controversial properties came to the fore of cutting edge research because they enable a new generation of photovoltaic devices. The continuous growth and development of the field is rapidly bringing a better understanding of their unconventional properties, but also raises a multitude of new questions regarding their fundamental properties. These materials promise further developments and expansion into other technological areas such as lasers, detectors, transistors, and LEDs. Their compositional diversity can produce a plethora of materials for which the optical absorption window can cover the whole range between near-UV and near-IR regions, and their electrical properties often can be tuned from metallic to insulating. Nevertheless, despite the enormous success of halide perovskites in photovoltaics, our current knowledge of the materials is limited and further work is required to unravel their secrets. Improved understanding of the defects and how they form will create new insights in controlling the optical, electronic, and charge-transport properties. Questions such as (i) "why is the PL emission of thin-films different from the bulk materials?", (ii) "is the quenching of the PL desirable in optoelectronic devices?", (iii) "what is the mechanism that makes the Sn-based perovskites metallic?", and (iv) "what is the origin of room temperature PL at 970 nm in tin-iodide perovskites that is sustained in the presence of good electrical conductivity?" need answers. Thus, we anticipate the main challenge in the future development of the compounds to be primarily synthetic, since current experience has shown that the various chemical and structural permutations in perovskites are not well controlled and often lead to inconsistent results. Therefore, high quality samples are a priority.

AUTHOR INFORMATION

Corresponding Author

*E-mail: m-kanatzidis@northwestern.edu.

Funding

This work was supported by the Department of Energy under Grant SC0012541. Use of the Advanced Photon Source at Argonne National Laboratory was supported by the U.S. Department of Energy, Office of Science, Office of Basic Energy Sciences, under Contract No. DE-AC02-06CH11357.

Notes

The authors declare no competing financial interest.

Biographies

Constantinos C. Stoumpos was born in Athens, Greece, in 1983. He completed his B.Sc. (2006) and Ph.D. (2009) degrees at the University of Patras in Greece, the latter under the supervision of Professor Spyros P. Perlepes, working on 3d-metal coordination chemistry relevant to molecular magnetism. He is a postdoctoral fellow at Northwestern University and at Argonne National Laboratory before that. His current research interests lie in the science and applications of halide perovskites.

Mercouri G. Kanatzidis was born in Greece in 1957. After obtaining a B.Sc. from Aristotle University in Greece, he received his Ph.D. in chemistry from the University of Iowa in 1984. He was a postdoctoral fellow at the University of Michigan and Northwestern University from 1985 to 1987 and is currently the Charles E. and Emma H. Morrison Professor of Chemistry at Northwestern University. He also holds an appointment at Argonne National Laboratory and is the editor in chief of the *Journal of Solid State Chemistry*.

REFERENCES

(1) Kojima, A.; Teshima, K.; Shirai, Y.; Miyasaka, T. Organometal Halide Perovskites as Visible-Light Sensitizers for Photovoltaic Cells. *J. Am. Chem. Soc.* **2009**, *131*, 6050−6051.

(2) Etgar, L.; Gao, P.; Xue, Z.; Peng, Q.; Chandiran, A. K.; Liu, B.; Nazeeruddin, M. K.; Grätzel, M. Mesoscopic $CH_3NH_3PbI_3/TiO_2$ Heterojunction Solar Cells. *J. Am. Chem. Soc.* **2012**, *134*, 17396−17399.

(3) Kim, H.-S.; Lee, C.-R.; Im, J.-H.; Lee, K.-B.; Moehl, T.; Marchioro, A.; Moon, S.-J.; Humphry-Baker, R.; Yum, J.-H.; Moser, J. E.; Gratzel, M.; Park, N.-G. Lead Iodide Perovskite Sensitized All-Solid-State Submicron Thin Film Mesoscopic Solar Cell with Efficiency Exceeding 9%. *Sci. Rep.* **2012**, *2*, 591.

(4) Lee, M. M.; Teuscher, J.; Miyasaka, T.; Murakami, T. N.; Snaith, H. J. Efficient hybrid solar cells based on meso-superstructured organometal halide perovskites. *Science* **2012**, *338*, 643−647.

(5) Chung, I.; Lee, B.; He, J.; Chang, R. P. H.; Kanatzidis, M. G. All-solid-state dye-sensitized solar cells with high efficiency. *Nature* **2012**, *485*, 486−489.

(6) Zhou, H.; Chen, Q.; Li, G.; Luo, S.; Song, T.-b.; Duan, H.-S.; Hong, Z.; You, J.; Liu, Y.; Yang, Y. Interface engineering of highly efficient perovskite solar cells. *Science* **2014**, *345*, 542−546.

(7) Jeon, N. J.; Noh, J. H.; Yang, W. S.; Kim, Y. C.; Ryu, S.; Seo, J.; Seok, S. I. Compositional engineering of perovskite materials for high-performance solar cells. *Nature* **2015**, *517*, 476−480.

(8) Goldschmidt, V. M. Die Gesetze der Krystallochemie. *Naturwissenschaften* **1926**, *14*, 477−485.

DOI: 10.1021/acs.accounts.5b00229
Acc. Chem. Res. 2015, 48, 2791−2802

(9) Shirwadkar, U.; van Loef, E. V. D.; Hawrami, R.; Mukhopadhyay, S.; Glodo, J.; Shah, K. S. New promising scintillators for gamma-ray spectroscopy: Cs(Ba,Sr) $(Br,I)_3$. *IEEE NSS/MIC Conference* **2011**, 1583−1585.
(10) Hesse, S.; Zimmermann, J.; von Seggern, H.; Ehrenberg, H.; Fuess, H.; Fasel, C.; Riedel, R. $CsEuBr_3$: Crystal structure and its role in the photostimulation of $CsBr:Eu^{2+}$. *J. Appl. Phys.* **2006**, *100*, 083506.
(11) Horowitz, A.; Amit, M.; Makovsky, J.; Dor, L. B.; Kalman, Z. H. Structure types and phase transformations in $KMnCl_3$ and $TlMnCl_3$. *J. Solid State Chem.* **1982**, *43*, 107−125.
(12) Im, J.-H.; Chung, J.; Kim, S.-J.; Park, N.-G. Synthesis, structure, and photovoltaic property of a nanocrystalline 2H perovskite-type novel sensitizer $(CH_3CH_2NH_3)PbI_3$. *Nanoscale Res. Lett.* **2012**, *7*, 353.
(13) Thiele, G.; Serr, B. R. Crystal structure of dimethylammonium triiodostannate(II), $(CH_3)_2NH_2SnI_3$. *Zeitschrift für Kristallographie* **1996**, *211*, 48.
(14) Wang, S.; Mitzi, D. B.; Feild, C. A.; Guloy, A. Synthesis and Characterization of $[NH_2C(I):NH_2]_3MI_5$ (M = Sn, Pb): Stereochemical Activity in Divalent Tin and Lead Halides Containing Single < 110> Perovskite Sheets. *J. Am. Chem. Soc.* **1995**, *117*, 5297−5302.
(15) Cao, D. H.; Stoumpos, C. C.; Farha, O. K.; Hupp, J. T.; Kanatzidis, M. G. 2D Homologous Perovskites as Light-Absorbing Materials for Solar Cell Applications. *J. Am. Chem. Soc.* **2015**, *137*, 7843−7850.
(16) Onoda-Yamamuro, N.; Yamamuro, O.; Matsuo, T.; Suga, H. p-T phase relations of $CH_3NH_3PbX_3$ (X = Cl, Br, I) crystals. *J. Phys. Chem. Solids* **1992**, *53*, 277−281.
(17) Lee, Y.; Mitzi, D. B.; Barnes, P. W.; Vogt, T. Pressure-induced phase transitions and templating effect in three-dimensional organic-inorganic hybrid perovskites. *Phys. Rev. B: Condens. Matter Mater. Phys.* **2003**, *68*, 020103.
(18) Woodward, P. Octahedral Tilting in Perovskites. I. Geometrical Considerations. *Acta Crystallogr., Sect. B: Struct. Sci.* **1997**, *53*, 32−43.
(19) Howard, C. J.; Stokes, H. T. Group-Theoretical Analysis of Octahedral Tilting in Perovskites. *Acta Crystallogr., Sect. B: Struct. Sci.* **1998**, *54*, 782−789.
(20) Darlington, C. Normal-mode analysis of the structures of perovskites with tilted octahedra. *Acta Crystallogr., Sect. A: Found. Crystallogr.* **2002**, *58*, 66−71.
(21) Stoumpos, C. C.; Malliakas, C. D.; Kanatzidis, M. G. Semiconducting tin and lead iodide perovskites with organic cations: phase transitions, high mobilities, and near-infrared photoluminescent properties. *Inorg. Chem.* **2013**, *52*, 9019−9038.
(22) Trots, D. M.; Myagkota, S. V. High-temperature structural evolution of caesium and rubidium triiodoplumbates. *J. Phys. Chem. Solids* **2008**, *69*, 2520−2526.
(23) Chung, I.; Song, J.-H.; Im, J.; Androulakis, J.; Malliakas, C. D.; Li, H.; Freeman, A. J.; Kenney, J. T.; Kanatzidis, M. G. $CsSnI_3$: Semiconductor or Metal? High Electrical Conductivity and Strong Near-Infrared Photoluminescence from a Single Material. High Hole Mobility and Phase-Transitions. *J. Am. Chem. Soc.* **2012**, *134*, 8579−8587.
(24) Hao, F.; Stoumpos, C. C.; Liu, Z.; Chang, R. P.; Kanatzidis, M. G. Controllable Perovskite Crystallization at a Gas-Solid Interface for Hole Conductor-Free Solar Cells with Steady Power Conversion Efficiency over 10%. *J. Am. Chem. Soc.* **2014**, *136*, 16411−16419.
(25) Jeon, N. J.; Noh, J. H.; Kim, Y. C.; Yang, W. S.; Ryu, S.; Seok, S. I. Solvent engineering for high-performance inorganic-organic hybrid perovskite solar cells. *Nat. Mater.* **2014**, *13*, 897−903.
(26) Dong, Q.; Fang, Y.; Shao, Y.; Mulligan, P.; Qiu, J.; Cao, L.; Huang, J. Electron-hole diffusion lengths > 175 μm in solution-grown $CH_3NH_3PbI_3$ single crystals. *Science* **2015**, *347*, 967−970.
(27) Shi, D.; Adinolfi, V.; Comin, R.; Yuan, M.; Alarousu, E.; Buin, A.; Chen, Y.; Hoogland, S.; Rothenberger, A.; Katsiev, K.; Losovyj, Y.; Zhang, X.; Dowben, P. A.; Mohammed, O. F.; Sargent, E. H.; Bakr, O. M. Low trap-state density and long carrier diffusion in organolead trihalide perovskite single crystals. *Science* **2015**, *347*, 519−522.
(28) De Wolf, S.; Holovsky, J.; Moon, S.-J.; Löper, P.; Niesen, B.; Ledinsky, M.; Haug, F.-J.; Yum, J.-H.; Ballif, C. Organometallic Halide Perovskites: Sharp Optical Absorption Edge and Its Relation to Photovoltaic Performance. *J. Phys. Chem. Lett.* **2014**, *5*, 1035−1039.
(29) Hao, F.; Stoumpos, C. C.; Chang, R. P. H.; Kanatzidis, M. G. Anomalous Band Gap Behavior in Mixed Sn and Pb Perovskites Enables Broadening of Absorption Spectrum in Solar Cells. *J. Am. Chem. Soc.* **2014**, *136*, 8094−8099.
(30) Ogomi, Y.; Morita, A.; Tsukamoto, S.; Saitho, T.; Fujikawa, N.; Shen, Q.; Toyoda, T.; Yoshino, K.; Pandey, S. S.; Ma, T.; Hayase, S. $CH_3NH_3Sn_xPb_{(1-x)}I_3$ Perovskite Solar Cells Covering up to 1060 nm. *J. Phys. Chem. Lett.* **2014**, *5*, 1004−1011.
(31) Im, J.; Stoumpos, C. C.; Jin, H.; Freeman, A. J.; Kanatzidis, M. G. Antagonism between spin-orbit coupling and steric effects causes anomalous band gap suppression in the perovskite photovoltaic materials $CH_3NH_3Sn_{1-x}Pb_xI_3$. *J. Phys. Chem. Lett.* **2015**, *6*, 3503−3509.
(32) Babin, V.; Fabeni, P.; Nikl, M.; Pazzi, G. P.; Sildos, I.; Zazubovich, N.; Zazubovich, S. Polarized luminescence of $CsPbBr_3$ nanocrystals (quantum dots) in CsBr:Pb single crystal. *Chem. Phys. Lett.* **1999**, *314*, 31−36.
(33) Xing, G.; Mathews, N.; Lim, S. S.; Yantara, N.; Liu, X.; Sabba, D.; Grätzel, M.; Mhaisalkar, S.; Sum, T. C. Low-temperature solution-processed wavelength-tunable perovskites for lasing. *Nat. Mater.* **2014**, *13*, 476−480.
(34) Zazubovich, S. Physics of halide scintillators. *Radiat. Meas.* **2001**, *33*, 699−704.
(35) Stoumpos, C. C.; Malliakas, C. D.; Peters, J. A.; Liu, Z.; Sebastian, M.; Im, J.; Chasapis, T. C.; Wibowo, A. C.; Chung, D. Y.; Freeman, A. J.; Wessels, B. W.; Kanatzidis, M. G. Crystal Growth of the Perovskite Semiconductor $CsPbBr_3$: A New Material for High-Energy Radiation Detection. *Cryst. Growth Des.* **2013**, *13*, 2722−2727.
(36) Borriello, I.; Cantele, G.; Ninno, D. Ab initio investigation of hybrid organic-inorganic perovskites based on tin halides. *Phys. Rev. B: Condens. Matter Mater. Phys.* **2008**, *77*, 235214.
(37) Tang, L. C.; Chang, Y. C.; Huang, J. Y.; Lee, M. H.; Chang, C. S. First Principles Calculations of Linear and Second-Order Optical Responses in Rhombohedrally Distorted Perovskite Ternary Halides, $CsGeX_3$ (X = Cl, Br, and I). *Jpn. J. Appl. Phys.* **2009**, *48*, 112402.
(38) Umari, P.; Mosconi, E.; De Angelis, F. Relativistic GW calculations on $CH_3NH_3PbI_3$ and $CH_3NH_3SnI_3$ Perovskites for Solar Cell Applications. *Sci. Rep.* **2014**, *4*, 4467.
(39) Huang, L.-y.; Lambrecht, W. R. L. Electronic band structure, phonons, and exciton binding energies of halide perovskites $CsSnCl_3$, $CsSnBr_3$, and $CsSnI_3$. *Phys. Rev. B: Condens. Matter Mater. Phys.* **2013**, *88*, 165203.
(40) Stoumpos, C. C.; Frazer, L.; Clark, D. J.; Kim, Y. S.; Rhim, S. H.; Freeman, A. J.; Ketterson, J. B.; Jang, J. I.; Kanatzidis, M. G. Hybrid Germanium Iodide Perovskite Semiconductors: Active Lone Pairs, Structural Distortions, Direct and Indirect Energy Gaps, and Strong Nonlinear Optical Properties. *J. Am. Chem. Soc.* **2015**, *137*, 6804−6819.
(41) Narayan, R. L.; Sarma, M. V. S.; Suryanarayana, S. V. Ionic conductivity of $CsPbCI_3$ and $CsPbBr_3$. *J. Mater. Sci. Lett.* **1987**, *6*, 93−94.
(42) Yamada, K.; Kuranaga, Y.; Ueda, K.; Goto, S.; Okuda, T.; Furukawa, Y. Phase Transition and Electric Conductivity of $ASnCl_3$ (A = Cs and CH_3NH_3). *Bull. Chem. Soc. Jpn.* **1998**, *71*, 127−134.
(43) Mitzi, D. B.; Feild, C. A.; Schlesinger, Z.; Laibowitz, R. B. Transport, Optical, and Magnetic Properties of the Conducting Halide Perovskite $CH_3NH_3SnI_3$. *J. Solid State Chem.* **1995**, *114*, 159−163.
(44) Mitzi, D. B.; Liang, K. Synthesis, Resistivity, and Thermal Properties of the Cubic Perovskite $NH_2CH{=}NH_2SnI_3$ and Related Systems. *J. Solid State Chem.* **1997**, *134*, 376−381.
(45) Takahashi, Y.; Hasegawa, H.; Takahashi, Y.; Inabe, T. Hall mobility in tin iodide perovskite $CH_3NH_3SnI_3$: Evidence for a doped semiconductor. *J. Solid State Chem.* **2013**, *205*, 39−43.
(46) Matsushima, T.; Fujita, K.; Tsutsui, T. Preparation of Conductive Organic-Inorganic Cubic Perovskite Thin Films by Dual-Source Vacuum Vapor Deposition. *Jpn. J. Appl. Phys.* **2006**, *45*, 523−525.

DOI: 10.1021/acs.accounts.5b00229
Acc. Chem. Res. 2015, 48, 2791−2802

(47) Scaife, D. E.; Weller, P. F.; Fisher, W. G. Crystal preparation and properties of cesium tin(II) trihalides. *J. Solid State Chem.* **1974**, *9*, 308−314.
(48) Valverde-Chávez, D. A.; Ponseca, C. J.; Stoumpos, C. C.; Yartsev, A.; Kanatzidis, M. G.; Sundström, V.; Cooke, D. G. Intrinsic femtosecond charge generation dynamics in a single crystal organometal halide perovskite. arXiv:1507.02179 [cond-mat.mtrl-sci]. arXiv.org e-Print archive. http://arxiv.org/abs/1507.02179, 2015.
(49) Noel, N. K.; Stranks, S. D.; Abate, A.; Wehrenfennig, C.; Guarnera, S.; Haghighirad, A.-A.; Sadhanala, A.; Eperon, G. E.; Pathak, S. K.; Johnston, M. B.; Petrozza, A.; Herz, L. M.; Snaith, H. J. Lead-free organic-inorganic tin halide perovskites for photovoltaic applications. *Energy Environ. Sci.* **2014**, *7*, 3061−3068.
(50) Kumar, M. H.; Dharani, S.; Leong, W. L.; Boix, P. P.; Prabhakar, R. R.; Baikie, T.; Shi, C.; Ding, H.; Ramesh, R.; Asta, M.; Graetzel, M.; Mhaisalkar, S. G.; Mathews, N. Lead-Free Halide Perovskite Solar Cells with High Photocurrents Realized Through Vacancy Modulation. *Adv. Mater.* **2014**, *26*, 7122−7127.
(51) Ponseca, C. S.; Savenije, T. J.; Abdellah, M.; Zheng, K.; Yartsev, A.; Pascher, T.; Harlang, T.; Chabera, P.; Pullerits, T.; Stepanov, A.; Wolf, J.-P.; Sundström, V. Organometal Halide Perovskite Solar Cell Materials Rationalized: Ultrafast Charge Generation, High and Microsecond-Long Balanced Mobilities, and Slow Recombination. *J. Am. Chem. Soc.* **2014**, *136*, 5189−5192.
(52) Hao, F.; Stoumpos, C. C.; Guo, P.; Zhou, N.; Marks, T. J.; Chang, R. P. H.; Kanatzidis, M. G. Solvent-Mediated Crystallization of $CH_3NH_3SnI_3$ Films for Heterojunction Depleted Perovskite Solar Cells. *J. AM. Chem. Soc.* **2015**, *137*, 11445−11452.
(53) Snaith, H. J.; Abate, A.; Ball, J. M.; Eperon, G. E.; Leijtens, T.; Noel, N. K.; Stranks, S. D.; Wang, J. T.-W.; Wojciechowski, K.; Zhang, W. Anomalous Hysteresis in Perovskite Solar Cells. *J. Phys. Chem. Lett.* **2014**, *5*, 1511−1515.

DOI: 10.1021/acs.accounts.5b00229
Acc. Chem. Res. 2015, 48, 2791−2802